Morphological, electrical and optical properties of Si-doped GaAs grown by MBE on GaAs non-(100)-oriented substrates

P. P. González-Borrero[a,b], M. V. Alves[b] and E. Marega Jr.[b]

[a]Departamento de Química e Física - UNICENTRO
85010-990 Guarapuava, PR - Brasil
gonzalez@unicentro.br

[b]Instituto de Física de São Carlos - USP
13560-970 São Carlos, SP - Brasil

(*Recebido: 22 de outubro de 2001*)

Abstract: *The incorporation and amphoteric behavior of Si has been investigated in molecular beam epitaxy (MBE) GaAs samples grown on (311)A, (211)A and (111)A substrates at different growth conditions. Hall effect measurements have revealed that the doping changes from p- to n-type when the* V_4/III *flux ratio is increased and the growth temperature is decreased. The transition flux ratio is lower for the (211)A than for the (311)A surfaces. Photoluminescence measurements have shown that, when the* V_4/III *flux ratio is increased or the growth temperature is decreased, arsenic vacancy defects are changed into pairs of Ga vacancy and Ga antisite defects. These results are explained by considering the kinetics of the MBE growth process and the orientation dependence of the surface bonding.*

Key words: *Si-doped GaAs; optical properties of Si-doped GaAs; GaAs non-(100)-oriented substrates*

Resumo: *A incorporação do Si e seu comportamento amfótero foi pesquisado utilizando a epitaxia por feixes moleculares (MBE) em amostras de GaAs crescidas em substratos (311)A, (211)A e (11)A a diferentes condições de crescimento. Medidas do efeito Hall mostraram que a dopagem varia do tipo* p *ao tipo* n *quando a razão do fluxo* V_4/III *é aumentada e a temperatura diminuída. A razão do fluxo de transição é menor para a superfície (211)A do que para a (311)A. Medidas de fotoluminescência mostraram que, quando a razão de fluxo* V_4/III *é aumentada ou a temperatura de crescimento diminuída, os defeitos de vacância*

no arsênio mudam para pares de defeitos de vacância do Ga e de anti-sítios do Ga. Esses resultados são explicados considerando-se a cinética do processo de crescimento por MBE e a dependência da orientação da superfície de ligação.

Palavras-chave: *GaAs dopado com Si; propriedades ópticas do GaAs dopado com Si; substratos de GaAs não orientados na direção (100).*

1 Introduction

In last years the investigation of the growth and doping of GaAs on non-(100)-oriented substrates has been attracting much interest because of both their distinctive physical properties related to crystallographic orientation and potentials for better performances [1]-[6]. The behavior of impurity incorporation during epitaxial growth depends on substrates orientation, and Si is widely used as an *n*-type dopant in conventional (100)-oriented GaAs growth using molecular beam epitaxy (MBE). However, Si behaves as an amphoteric dopant in (N11)A-oriented GaAs. The conduction type of Si-doped GaAs grown by MBE on an GaAs(N11)A-oriented substrate can be controlled by adjusting growth conditions. It has been reported that Si shows a *p*-type conductivity in (N11)A-oriented GaAs when $N \leq 3$, whereas it changes to an *n*-type when $N > 3$ [7, 8].[1]

In this work, we present a study of the Si-doping characteristics of GaAs grown on (N11)A-substrates (N=1, 2 and 3) as a function of growth conditions: V_4/III flux ratio and growth temperature. By means of the comparison of electrical and luminescence measurements we have studied the role of optically active point defects in determining the conversion of the doping from *p* to *n* type.

2 Experimental

We have grown Si-doped GaAs as function of growth temperature and V_4/III flux ratio on semi-insulating GaAs substrates with different orientations. Before growth, the native oxide layer was removed with H_2SO_4 and the wafers were etched with $NH_4 : H_2O_2 : H_2O$ (2:1:95) etched for 2 min. at 25 °C [9].

The samples were immediately mounted on a molybdenum block and loaded into an MBE system (MECA 2000). The (100)-oriented GaAs substrates were also mounted on the same Mo block for reference purpose. The conventional Ga and As_4 molecules from solid sources were use for the growth. After thermal cleaning at 620 ^{o}C for 5 min., a 100-nm-thick undoped GaAs buffer layer, a superlattice $(AlAs)_5/(GaAs)_{10}$[2] with period 10 and a 200-nm-thick undoped GaAs buffer layer were successively grown at 600 ^{o}C. After this, a 500-nm-thick Si-undoped GaAs layer was grown at different growth temperatures, under various V_4/III flux ratios

[1] The notation A or B is used to differentiate the atomic termination of the polar (N11) surfaces: A is Ga terminated and B is As terminated.

[2] The numbers denote the thicknesses of the corresponding layers expressed in monolayers (ML).

between 3 and 33. The Si effusion cell temperature was chosen such that the target Si concentration was 1×10^{18}cm^{-3} in (100) grown GaAs under normal growth conditions.

The Ga and As fluxes were calibrated using reflection high-energy electron diffraction (RHEED) intensity oscillations on a GaAs(100) substrate. Growth temperatures were measured using a termocouple referenced to the c(4x4) to (2x4) surface reconstruction change on the GaAs(100) at 520°C under an As_4 flux of 2 ML/s.

The surface morphologies were observed by Nomarski interference microscope with a maximum magnification of 1000x. Van der Pauw Hall measurements at room temperature were used to determine the doping type and the free-carrier concentration of the grown samples. Photoluminescence (PL) measurements at 25 K using an argon-ion laser (514.5 nm) line as an excitation source were also carried out for optical characterizations. The PL spectra were recorded by lock-in amplifier techniques, and the excitation power density was about 6 W/cm^2.

3 Results and Discussion

3.1 Surface morphology

The superficial macroscopic morphology of the grown samples was investigated using interference Nomarski microscope with amplification of 1000x. For the GaAs(100), no significant change in the macroscopic surface morphology is observed over the entire range studied here (not shown). Figure 1 shows the superficial morphology of the GaAs:Si samples grown on GaAs(111)A surface under V_4/III flux ratios of 3.8(a), 6.3(b) and 21(c) at a growth temperature of 550°C. For low flux ratio, it is possible to see defects on the surface. The defect density decreases when the flux ratio increases. Then, only growth at high V_4/III ratios and low temperatures produces flat surfaces on the (111)A oriented samples. As the growth temperature was raised or the V_4/III ratio was lowered, the surface morphology degraded.

Nomarski optical micrograph images show good surface morphologies of Si-doped GaAs grown on GaAs(311)A substrates under all growth conditions, even in growth under Ga-rich conditions (see Fig. 2). This result is in strong contrast to the case of the Si-doped GaAs(111)A, in which the growth condition (conduction-type) shows a clear correlation with macroscopic surface morphology.

On the other hand, GaAs:Si superficial morphology of samples grown on GaAs(211)A planes depend on the growth conditions. Usually these samples show a cloudy surface when they are observed by naked eye. When they are characterized by means of a microscope, superficial defects are revealed. In figure 3 are shown the surfaces of GaAs:Si/GaAs(211)A for three different growth temperature under a constant V_4/III flux ratio of 5.4. The best surface was obtained at 550°C for this flux ratio. This sample shows a mirror-like surface by naked-eye observation, but when it was studied by means of a microscope, the presence of a low defect density on the surface was detected.

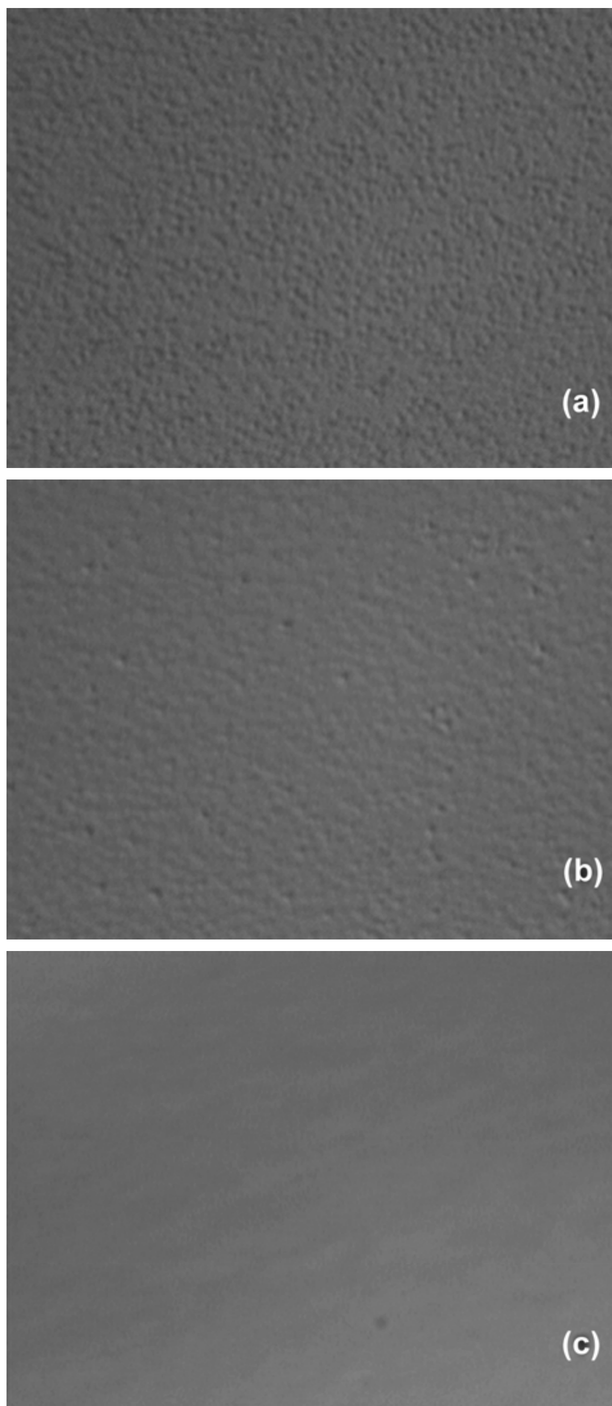

Figure 1. Nomarski interference viewgraphs of Si-doped GaAs layers grown on (111)A substrates at a constant growth temperature of 550°C under different flux ratio: (a) 3.8, (b) 6.3, and (c) 21.

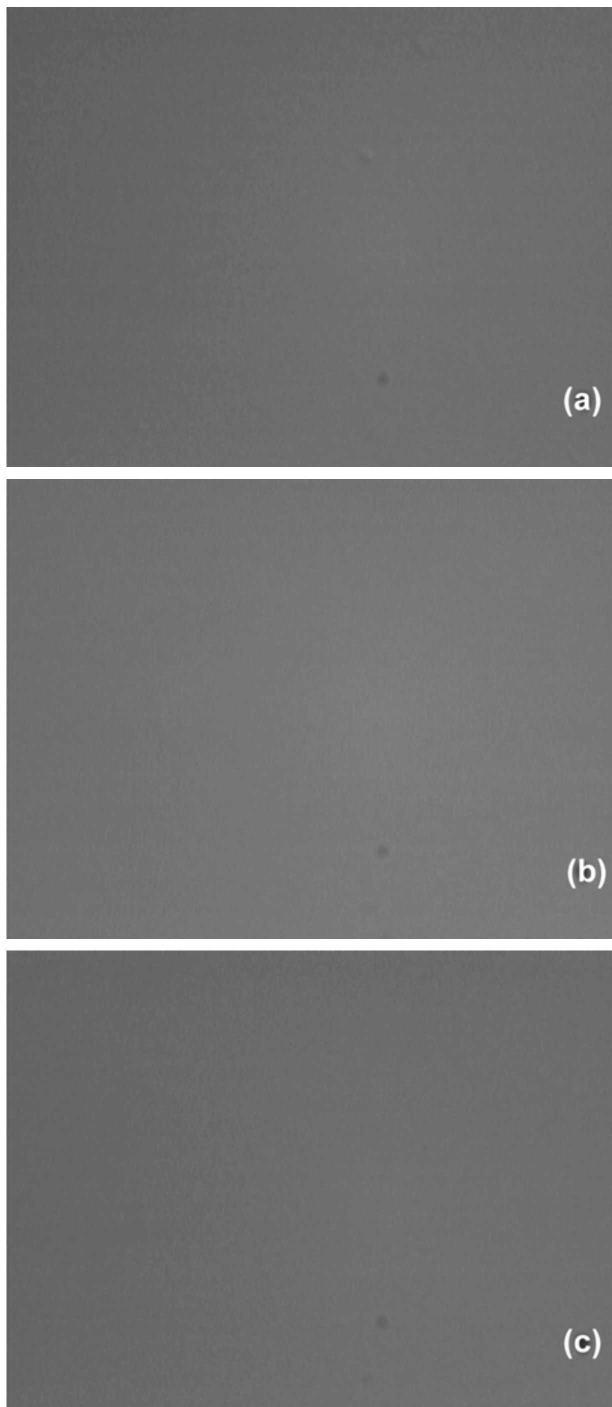

Figure 2. Nomarski optical micrograph images of Si-doped GaAs layers grown on (311)A surfaces at $T_g = 650$ (a), 500 (b), and 420°C (c) under a constant V_4/III flux ratio of 4.5.

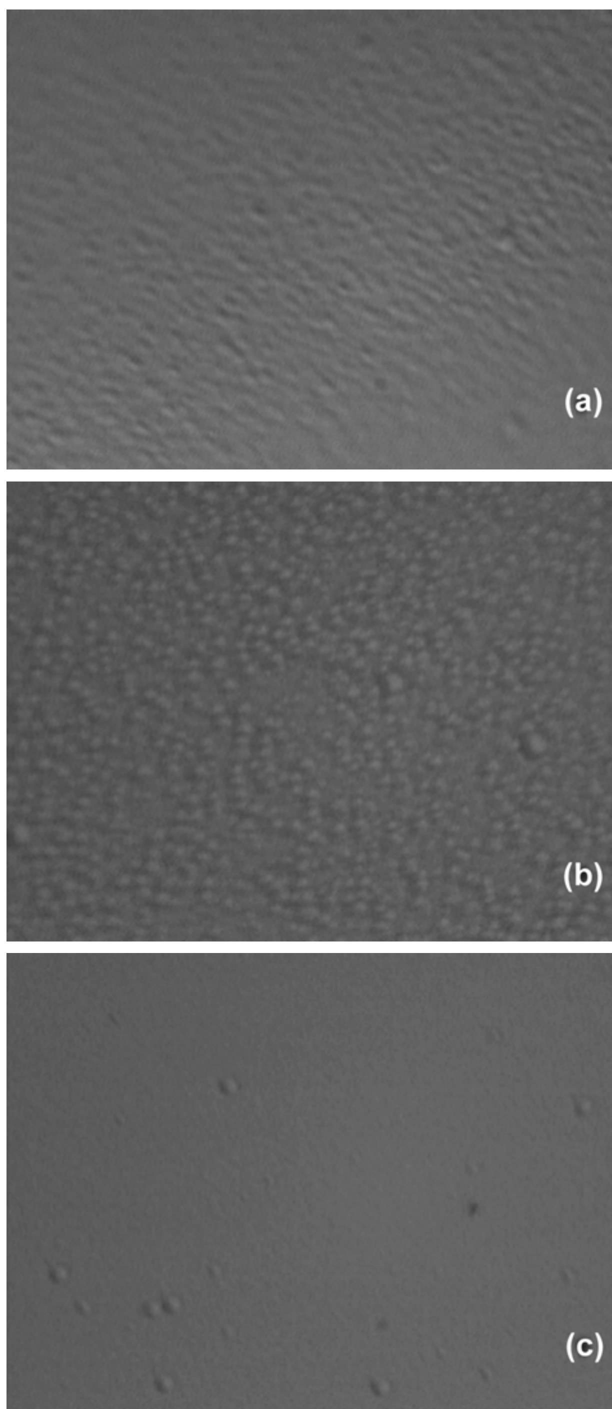

Figure 3. Nomarski interference pictures of the surface morphologies of the (111)A GaAs grown at $T_g = 620$ (a), 580 (b), and 550°C (c) under a constant V_4/III flux ratio of 5.4.

3.2 Electrical characterization

Van der Pauw Hall measurements at room temperature were used to determine the doping type and the free-carrier concentration of the growth samples. The doping characteristics of Si in GaAs depend on growth conditions and substrate orientations. In Fig. 4, a summary of the free-carrier concentration and the doping type is shown as a function of growth temperature (T_g) and V_4/III flux ratio.

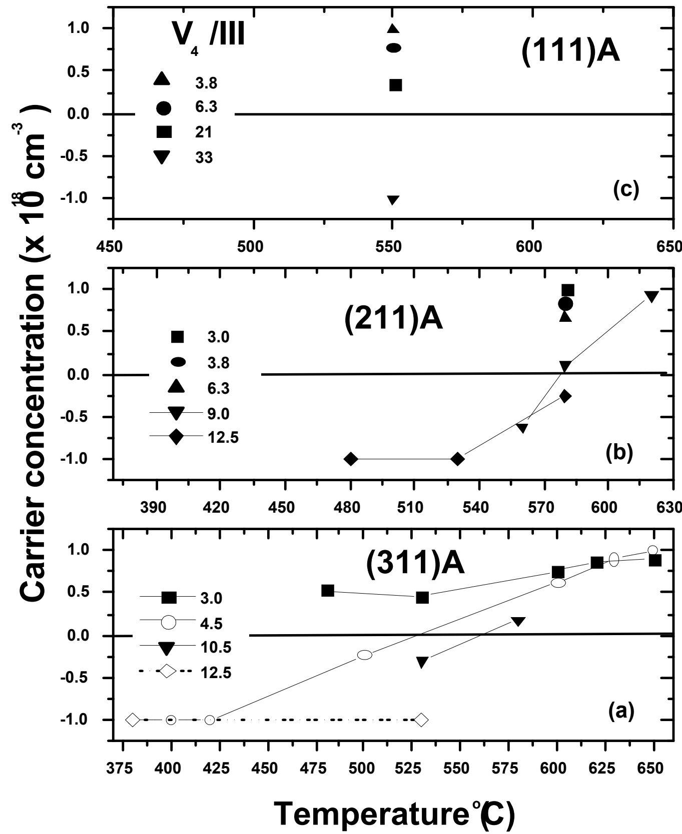

Figure 4. Carrier concentration of Si-doped GaAs grown on (a) GaAs(311)A, (b) (211)A, and (c) (111)A surfaces as a function of the growth temperature and V_4/III flux ratio. A negative and positive sign for carrier concentration indicate *n* and *p* type, respectively. The lines are only guides for the eyes.

As shown in Fig. 4(a), the Si-doped GaAs(311)A tends to exhibit *p*-type conduction at higher T_g and/or lower V_4/III, while it tends to be *n*-type at lower T_g and/or higher V_4/III. Conversion of conduction type from *p* to *n* type was observed in these samples at a high growth temperature of more than 530°C by increasing a V_4/III flux ratio. Near the boundary some of the samples became highly resistive, showing neither *p*- nor *n*-type conduction, due to the autocompensation effect. The

experimental results suggest that the transition occurs at a lower flux ratio for the (211)A samples compared to the (311)A samples (see Fig. 4(b)).

On the other hand, the doping characteristics of Si in GaAs(111)A are different from those in GaAs(211)A and GaAs(311)A. Si behaves as an acceptor over the wide growth condition range as shown in Fig. 4(c).

From figure 4, we can also see the activation efficiency of Si η. For the three orientations, the activation efficiencies η in both n- and p-type regions are high, except for the transition region. On the contrary, Si-doped GaAs(100) samples always show an n-type conduction with $\eta \simeq 100\%$ (not shown here); no significant dependence of the electrical properties on the growth condition was observed within the experimental range studied here.

In the cases of Si-doped GaAs samples grown on (111)A and (211)A planes, the conduction type has a strong correlation with the surface morphology; samples with flat surfaces show n-type conduction, whereas samples with rough surfaces are p type.

3.3 Optical characterization

A summary of the PL spectra for the (311)A, (211)A and (111)A samples are reported in figures 5, 6 and 7, respectively. For the p-type samples, grown at low V_4/III flux ratio and high T_g, it is possible to see a high-intensity peak around 1.48 eV. This peak is due to the band-to-band (BB) emission of a hole gas with electrons in the conduction band [10]. At about 1.45 eV, there is emission due to the recombination of an electron bound to an As vacancy with a hole bound to a Si_{As} acceptor level [11]. The presence of As vacancies (V_{As}) is expected due to the low V_4/III flux ratio used in the growth.

For the n-type samples ($\simeq 1 \times 10^{18}$ cm^{-3}), grown at high V_4/III flux ratio, the PL spectrum is characterized by a wide peak centered at about 1.49 eV, 1.50 eV, and 1.51 eV for (311)A, (111)A and (211)A surfaces, respectively. These emissions are attributed to the band-to-band (e-h) recombination [10] and to the recombination of electrons in the renormalized conduction band, with holes on deep acceptor levels [12]. The low energy side of spectra is probably due to the overlapping emissions of a donor-to-acceptor (=carbon) recombination (e-A) and to the band-tailing effect. The association of these emissions with point defects is also suggested by their linewidth.

At high energy, a shoulder is observed on this band for the (211)A samples. This shoulder is the so-called Mahan peak and is an enhancement of the luminescence transition at the Fermi energy due to the electron-hole correlation. Therefore, this shoulder is due to Mahan's excitons, which are quasi-bound states formed by electron and hole at the Fermi energy [13]-[15]. In the case of the (311)A samples, a well defined PL peak is observed at about 1.51 eV. Such peak is attributed to a neutral-acceptor bound-exciton emission (A^o, X) [16]. This emission was also observed for (111)A surface at about 1.50 eV.

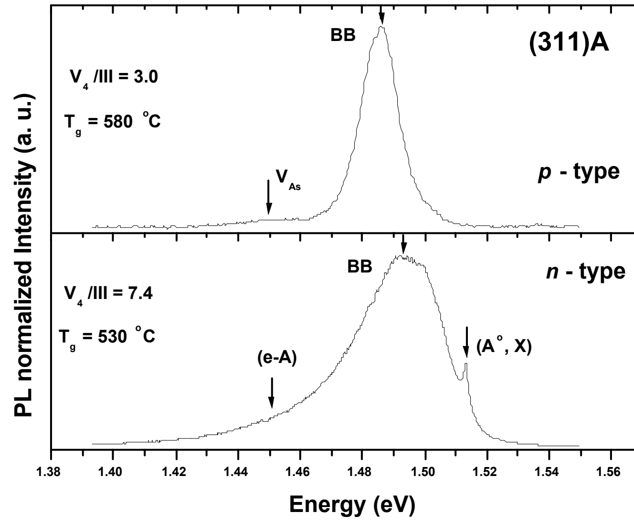

Figure 5. PL normalized spectra of GaAs(311)A samples measured at 25 K. On each spectrum the free-carrier type, growth temperature (T_g), and V_4/III flux ratio used during the growth are indicated. The labels on the spectra refer to the different recombination processes and means: BB band-to-band, V_{As} As vacancy, (A^o, X) neutral-acceptor bound-exciton, and (e-A) donor-to-acceptor.

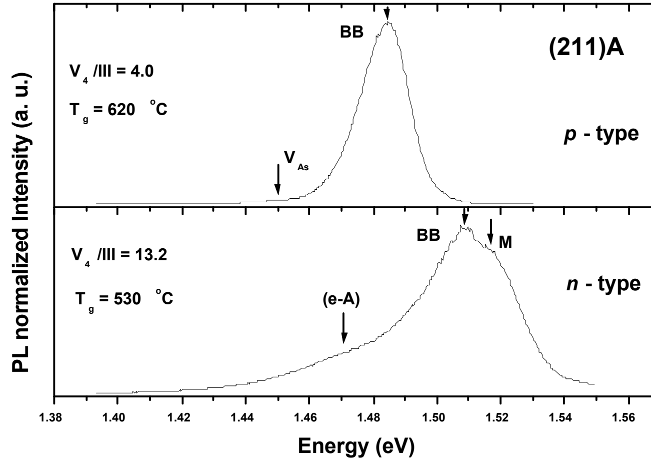

Figure 6. PL normalized spectra of GaAs(211)A samples measured at 25 K. On each spectrum the free-carrier type, growth temperature (T_g), and V_4/III flux ratio used during the growth are indicated. The labels on the spectra refer to the different recombination processes and means: BB band-to-band, V_{As} As vacancy, and M Mahan peak.

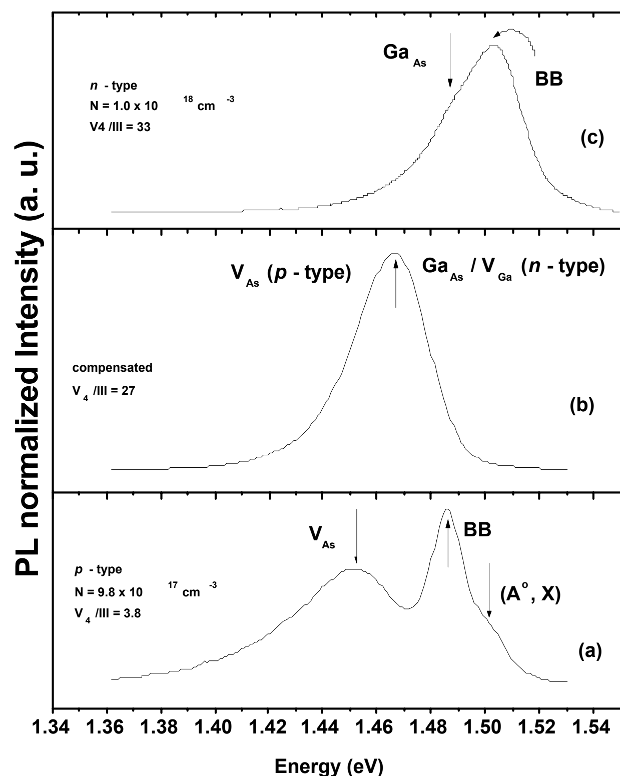

Figure 7. PL normalized spectra of GaAs(111)A samples measured at 25 K. On each spectrum the free-carrier type, and V_4/III flux ratio used during the growth at 550^oC are indicated. The labels on the spectra have the same meaning as in figures 5 and 6. V_{Ga} and Ga_{As} refer to emission through Ga vacancy and Ga antisite, respectively.

Other information is obtained from PL measurements at low temperature. The figures 8 and 9 show PL normalized spectra for the (211)A surface as a function of growth temperature and V_4/III flux ratio, respectively. The optical-property behavior of the grown samples for the different growth conditions can be explained by the following defect reaction:

$$V_{As} \longleftrightarrow V_{Ga} + Ga_{As} \tag{1}$$

where an As vacancy transforms into a pair of Ga antisite and Ga vacancy with a single Ga atom hop [17]. Because these defects are charged, the reaction is driven by the Fermi level position. The single Ga atom hop is favored in n-type samples and changes a deep donor (V_{As}) into a pair of deep acceptors (V_{Ga} and Ga_{As}). Also the increase in the V_4/III flux ratio drives the reaction to the left side.

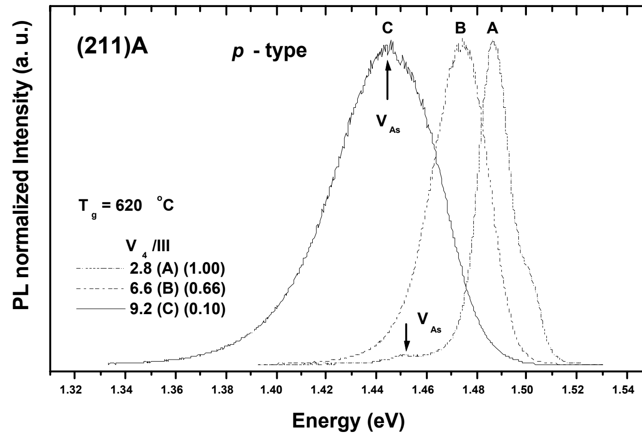

Figure 8. PL normalized spectra of p-type GaAs(211)A samples at 25 K. These samples were grown at $T_g = 620^oC$. The spectra identified by A, B and C correspond to a V_4/III flux ratio of 2.8, 6.6, and 9.4, respectively. The values in parentheses indicate the free-carrier concentration (in units of 10^{18} cm^{-3}). V_{As} refers to recombination through As vacancies. The spectra behavior is explained in text.

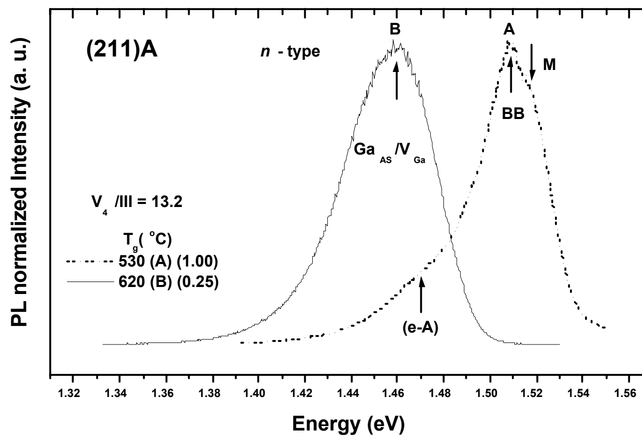

Figure 9. PL normalized spectra of n-type GaAs(211)A samples at 25 K. The samples were grown under V_4/III flux ratio of ∼13.2 at different temperatures. The spectra identified by A and B refer to $T_g = 530$ and 620° C, respectively. The values in parentheses indicate the free-carrier concentration (in units of 10^{18} cm^{-3}). The labels on the spectra have the same meaning as in figures 6 and 7. The spectra behavior is explained in text.

During the MBE growth of GaAs, the lattice site where Si incorporates is determined by the balance between the Si-Ga and Si-As bond strengths, the available surface energy to break the As_4 molecules to yield atomic As and the As surface coverage [18]. In addition, the (211)A and (311)A surfaces are composed of steps with (111)A and (100) orientations. The (211)A surface has two atoms in the (111)A steps and one atom in the (100) steps, while the (311)A surface has one atom per step. In the (100) surface, each Ga or As atom has two back-bonds to the substrate, whereas, in the (111)A surface, the As atoms have only one back-bond to the substrate while the Ga atoms have three back-bonds.

During the growth, the available As sites on the (111) surface have a low valence charge density (single dangling bonds), i.e. a low energy is available for breaking the impinging As_4 molecules [18]. As a consequence, at low V_4/III flux ratio this favors the formation of V_{As} and the incorporation of Si on As sites, where it acts as an acceptor (see Fig. 7(a)). PL data shows both the effect of *p*-type doping and the emission due to V_{As}.

The increase of the V_4/III flux ratio during the growth causes the As surface coverage to increase, and consequently, the incorporation of As increases. This leads to a decrease in the concentration of As vacancies and, according to eq. 1, a large density of Ga vacancies forms. Si fills up both As and Ga vacancies, leaving behind a large number of Ga antisite defects and the samples highly compensated. The PL spectra are mainly dominated by deep defect emission of the Ga_{As} type while no band-to-band emission is observed (see Fig. 7(b)).

As the V_4/III flux ratio is further increased a negligible number of V_{As} forms, eq. 1 is completely driven to the left side and there is now a large production of Ga vacancies and Ga antisite defects. Si mainly incorporates on the Ga sites (where it acts as a donor). The Si doping thus changes from p to n type and we observe a low compensation for all sample orientations (see Fig. 7(c)).

Other characteristic observed in PL spectra is related with peak-position dependence on growth conditions. For *p*-type samples, the peak-position shift to lower energy with V_4/III flux-ratio increase at fixed growth temperature. Moreover, a broadening of these peaks is induced by a local potential fluctuation and by the presence of defects in these growth conditions (see Fig. 8).

In the case of *n*-type samples (see Fig. 9), the substrate temperature increase for a fixed V_4/III flux ratio causes a peak-position shift to lower energy and a broadening of PL peak. For *p*-type samples, the peak located at about 1.45 eV is attributed to V_{As} related emission, whereas it is attributed to a gallium antisite defect Ga_{As} or V_{Ga} related emission for *n*-type samples [19, 20].

The PL peak-position shift to lower energy, in both cases, is related to a decrease of the free-carrier concentration. In Fig. 8, an V_4/III increase and/or T_g decrease (from sample C) induce a change from *p*- to *n*-type conductivity. On the other hand, for samples in Fig. 9, an additional T_g increase and/or V_4/III decrease induce a change from *n*- to *p*-type. For the (311)A, (111)A surfaces, a similar behavior was observed in the optical properties of the *p*- and *n*-type samples. The different V_4/III flux-ratio and T_g values between the (311)A and (211)A surfaces for the conversion

from *p*- to *n*-type are probably because the dangling bond density on these planes is 52% and 71% of the dangling bond density of the (111)A surface for the (311)A and (211)A surfaces, respectively [21].

4 Summary

We have studied the superficial macroscopic morphologies, and the electrical and optical properties of MBE-grown Si-doped GaAs(N11)A layers, N = 1, 2 and 3. The changeover of Si impurity from being an acceptor to a donor in these oriented substrates has been investigated. An increase in the V_4/III flux ratio and/or decrease in T_g during growth induces a site switching of Si from an As site to a Ga site. This conversion from *p*- to *n*-type behavior coincides with a change in the main point defect present in the sample: As vacancy (V_{As}) for low V_4/III flux ratio and/or high growth temperature and Ga vacancy (V_{Ga}) for high V_4/III flux ratio and/or low growth temperature. A dependence of transition V_4/III flux ratio and growth temperature on the surface orientation has been observed and is attributed to the different dangling bond densities of the surfaces.

Acknowledgments

The authors would like to thank FAPESP-Brazil for financial support.

References

[1] T. Hayakawa, K. Takahashi, M. Kondo, T. Suyama, S. Yamamoto, and T. Hijikata, *Physical Review Letters* 60, 349 (1988).

[2] Y. Nakamura, M. Tsuchiya, S. Koshiba, H. Noge, and H. Sakaki, *Applied Physic Letters* 64, 2552 (1994).

[3] J. L. Sánchez-Rojas, A. Sacedón, F. Calle, E. Calleja, and E. Muñoz, *Applied Physic Letters* 65, 2042 (1994).

[4] N. R. Gardner, P. S. Domínguez, and J. J. Harris, *Semicond. Sci. Techol.* 12, 1583 (1997).

[5] W. Ma, R. Nötzel, M. Ransteiner, U. Jahn, H. P. Schönherr, H. Kostial, and H. Ploog, *Applied Physics Letters* 75, 1836 (1999).

[6] R. Nötzel, and K. H. Ploog, *Applied Surface Science* 166, 406 (2000).

[7] J. M. Ballingall and C. E. C. Wood, *Applied Physic Letters* 41, 947 (1982).

[8] W. I. Wang, E. E. Mendez, T. S. Kuan, and L. Esaki, *Applied Physic Letters* 47, 826 (1985).

[9] T. Yamamoto, M. Inai, T. Takebe, and T. Watanabe, *Journal of Vacuum Science & Technology A* 11, 631 (1993).

[10] G. Borgs, K. Bhattachryya, K. Deneff, P. V. Mieghen, and R. Mertens, Journal of Applied Physics 66, 4381 (1980).

[11] H. Birey, and J. Sites, *Journal of Applied Physics* 51, 619 (1980).

[12] L. Pavesi, and M. Guzzi, *Journal of Applied Physics* 75, 4779 (1994).

[13] N. H. Ky, L. Pavesi, D. Araujo, J. D. Ganiére, and F. K. Stievenard, J*ournal of Applied Physics* 64, R65 (1988).

[14] A. Haufe, R. Schwabe, H. Fieseler, and M. Ilegems, *Journal of Physics C: Solid State Physics* 21, 2951 (1988).

[15] G. D. Mahan, Physical Review 153, 882 (1967).

[16] E. H. Bogardus, and H. B. Bebb, *Physical Review* 176, 993 (1968).

[17] G. A. Baraff, and M. Schlutter, *Physical Review B* 33, 7346 (1986).

[18] B. Lee, S. S. Bose, M. H. Kim, A. D. Reed, G. E. Stillman, W. I. Wang, L. Vina, and P. C. Colter, *Journal of Crystal Growth* 96, 27 (1989).

[19] A. A. Bonapasta, B. Bonani, M. Capizzi, L. Cherubini, V. Emiliani, A. Frova, and F. Sarto, *Journal of Applied Physics* 73, 3326 (1993).

[20] M. Bugajski, K. H. Ko, J. Lagowski, and H. C. Gatos, *Journal of Applied Physics* 65, 596 (1989).

[21] D. J. Chadi, *Physical Review B* 29, 785 (1984).